

Electronic Supplementary Information for:

**Magnetic interactions controlled by light in the family of Fe(II)-  
M(IV) (M = Mo, W, Nb) hybrid organic-inorganic frameworks**

Michał Magott<sup>a,\*</sup>, Magdalena Ceglarska<sup>b</sup>, Michał Rams<sup>b</sup>, Barbara Sieklucka<sup>a</sup>, Dawid Pinkowicz<sup>a</sup>

<sup>a</sup> *Jagiellonian University, Faculty of Chemistry, Gronostajowa 2, 30-387 Kraków, Poland*

<sup>b</sup> *Jagiellonian University, Institute of Physics, Łojasiewicza 11, 30-348 Kraków, Poland*

### Structure determination

The single crystal X-ray diffraction data for **Fe<sub>2</sub>Mo** and **Fe<sub>2</sub>W** were collected using Bruker D8 Quest Eco Photon 50 CMOS diffractometer equipped with Mo K $\alpha$  radiation source (sealed tube) and a graphite monochromator. Absorption correction, data reduction and unit cell refinement were performed using SADABS and SAINT programs included in the Apex3 suite. Diffraction experiments for **Fe<sub>2</sub>Nb** were performed at the European Synchrotron Radiation Facility using synchrotron radiation at the Swiss-Norwegian beamline BM01 (experiment no. SC-4651). Absorption correction, data reduction and unit cell refinement were performed using SCALE3 ABSPACK and CrysAlis RED software. The structures were solved using direct methods and refined anisotropically using weighted full-matrix least-squares on  $F^2$ .<sup>1-3</sup> Hydrogen atoms were treated by a mixture of independent and constrained refinement. Structural diagrams were prepared using Mercury CSD 2020.3.0.<sup>4</sup>

### Powder X-ray diffraction

PXRD data were obtained using Bruker D8 Advance diffractometer (Cu K $\alpha$  radiation, graphite monochromator) at room temperature for ground crystalline samples under mother solution, which were loaded into glass capillaries (0.7 mm in diameter). Results were subjected to background correction using the DIFFRAC algorithm implemented in the DIFFRAC.EVA V5 software.

### Infrared spectroscopy

Infrared spectra were recorded using a Nicolet iN10 MX FT-IR microscope in the transmission mode (a small amount of powdered sample was spread on a BaF<sub>2</sub> pellet).

### UV-Vis spectroscopy

UV-Vis spectra were measured in transmission mode for samples mixed with paraffin oil between two quartz slides using a Shimadzu UV-3600i Plus spectrophotometer equipped with an integrating sphere.

### Magnetic and photomagnetic measurements

Magnetic susceptibility measurements were performed using a Quantum Design MPMS-3 Evercool magnetometer or a Quantum Design MPMS-XL magnetometer. All the samples were packed into glass tubes under a small amount of mother solution. The experimental data were corrected for the diamagnetism of the sample and the sample holder. Photomagnetic measurements were performed for samples ( $\approx 0.1$  mg) placed between two layers of adhesive tape and inserted into the plastic straw. They were inserted into the magnetometer and evacuated at 240 K in order to avoid dehydration. Irradiation was performed using 450 nm light produced by a laser diode (L450P1600MM; power at the sample position 6-10 mW/cm<sup>2</sup>).

### Specific heat measurements

Specific heat was measured using Quantum Design PPMS. Samples were pressed into pellets with no binder (**Fe<sub>2</sub>Mo** and **Fe<sub>2</sub>Nb**) or crystals were mixed with Apiezon N without crushing crystals (**Fe<sub>2</sub>W**). Apiezon N grease was used to ensure the thermal contact with the microcalorimeter. The heat capacity of the microcalorimeter with the grease was measured prior to the sample measurement and subtracted. The sample chamber was evacuated at 240 K. In the vicinity of the phase transitions, raw temperature relaxation  $T(t)$  curves were post-processed to achieve denser data points.

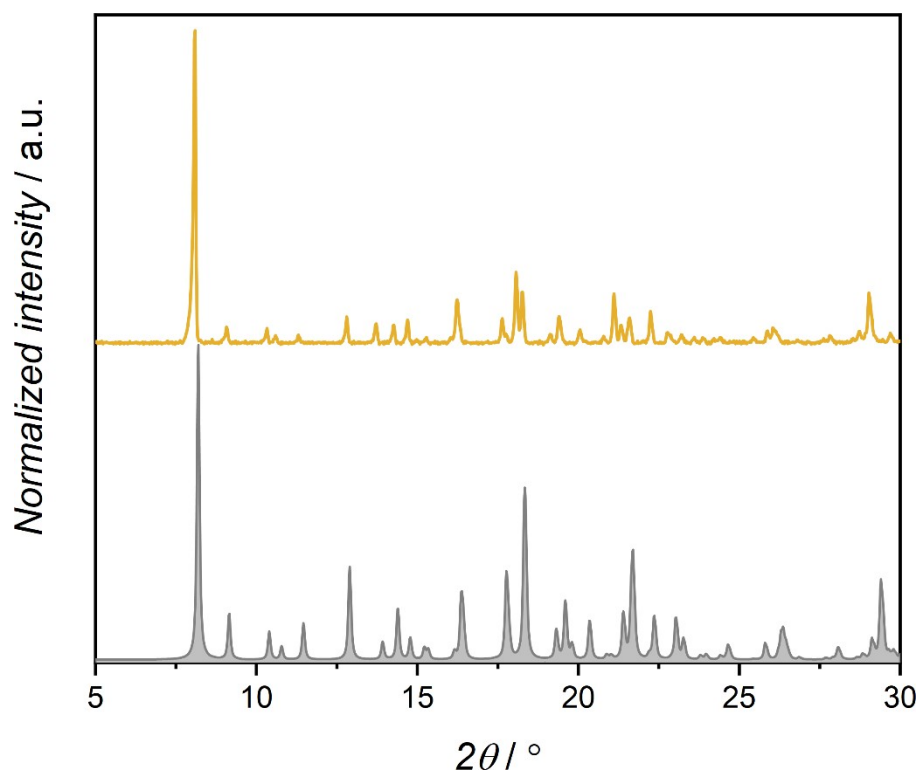


**Figure S1.** Powder X-ray diffraction pattern obtained for  $\text{Fe}_2\text{Mo}$  at room temperature (yellow line) and calculated for single-crystal structure at 120 K (grey line). Slight differences are due to the thermal shifts.

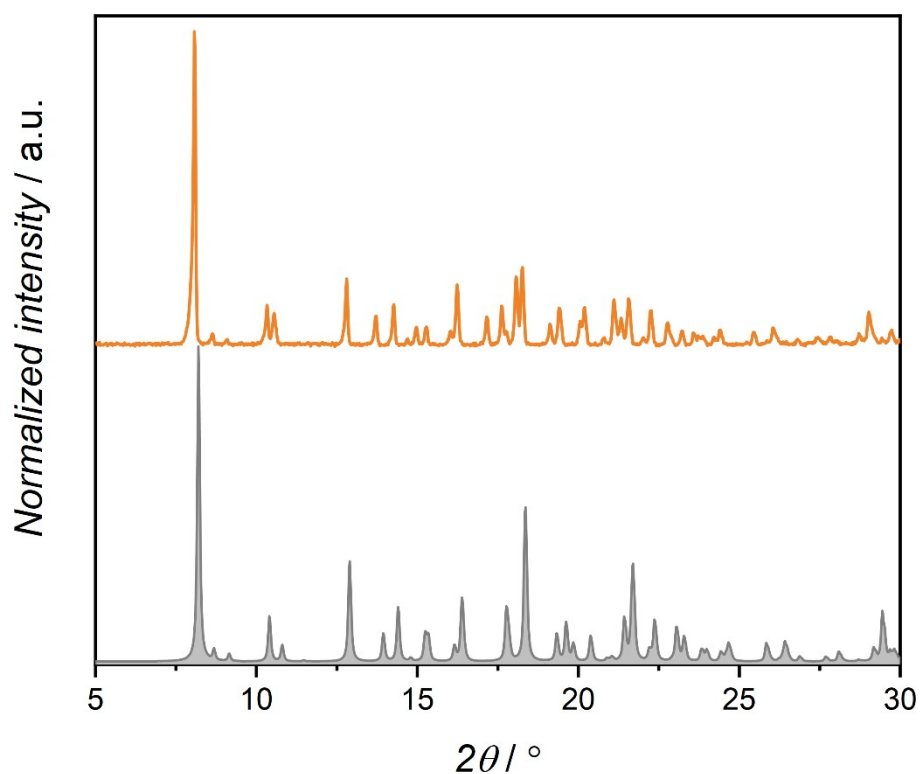


**Figure S2.** Powder X-ray diffraction pattern obtained for  $\text{Fe}_2\text{W}$  at room temperature (yellow line) and calculated for single-crystal structure at 120 K (grey line). Slight differences are due to the thermal shifts.

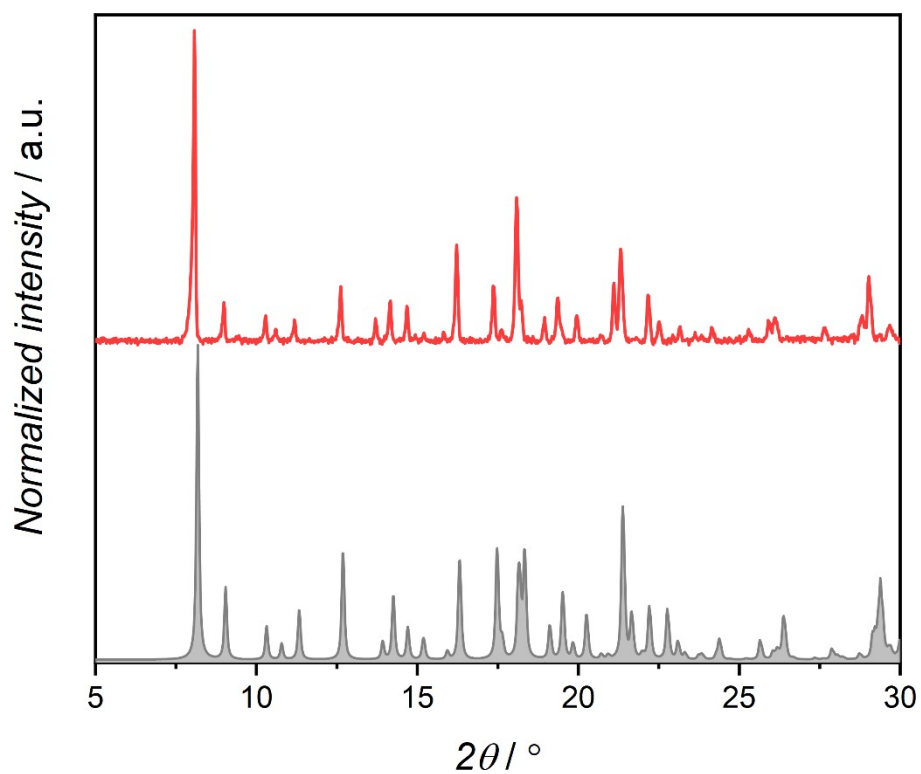


**Figure S3.** Powder X-ray diffraction pattern obtained for  $\text{Fe}_2\text{Nb}$  at room temperature (yellow line) and calculated for single-crystal structure at 100 K (grey line). Slight differences are due to the thermal shifts.

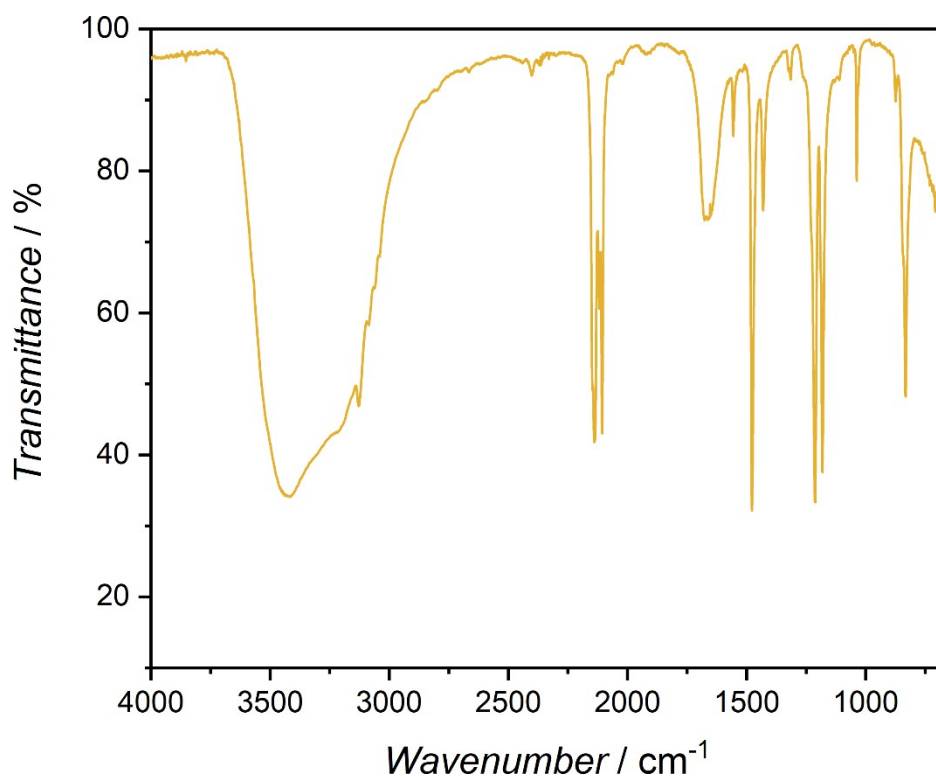


**Figure S4.** Infrared spectrum obtained for  $\text{Fe}_2\text{Mo}$ .

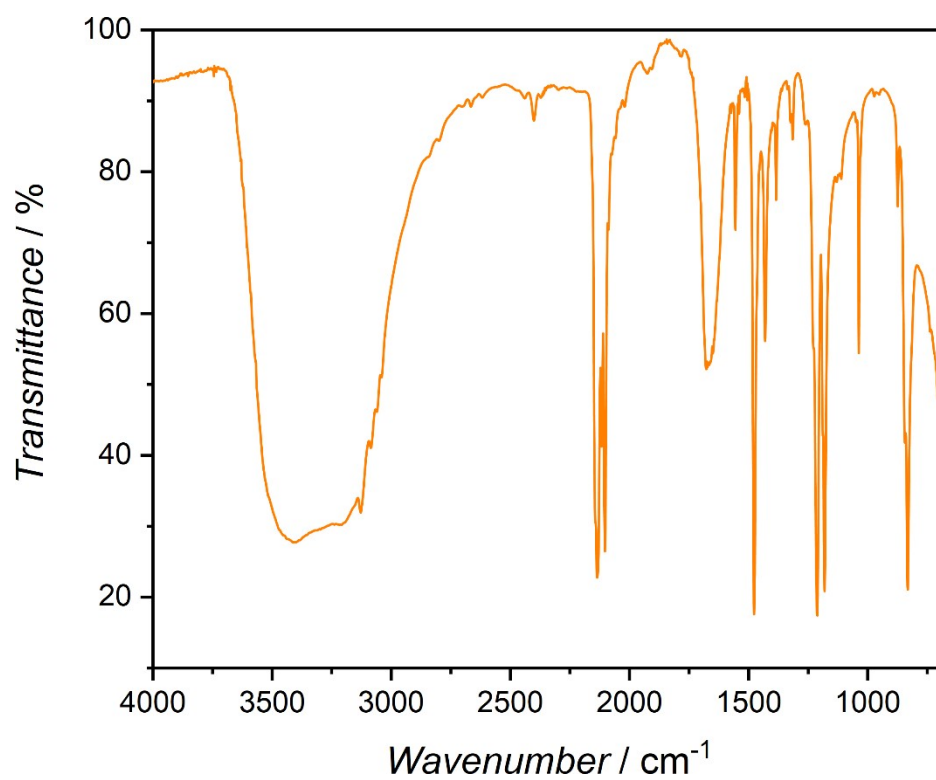


**Figure S5.** Infrared spectrum obtained for  $\text{Fe}_2\text{W}$ .

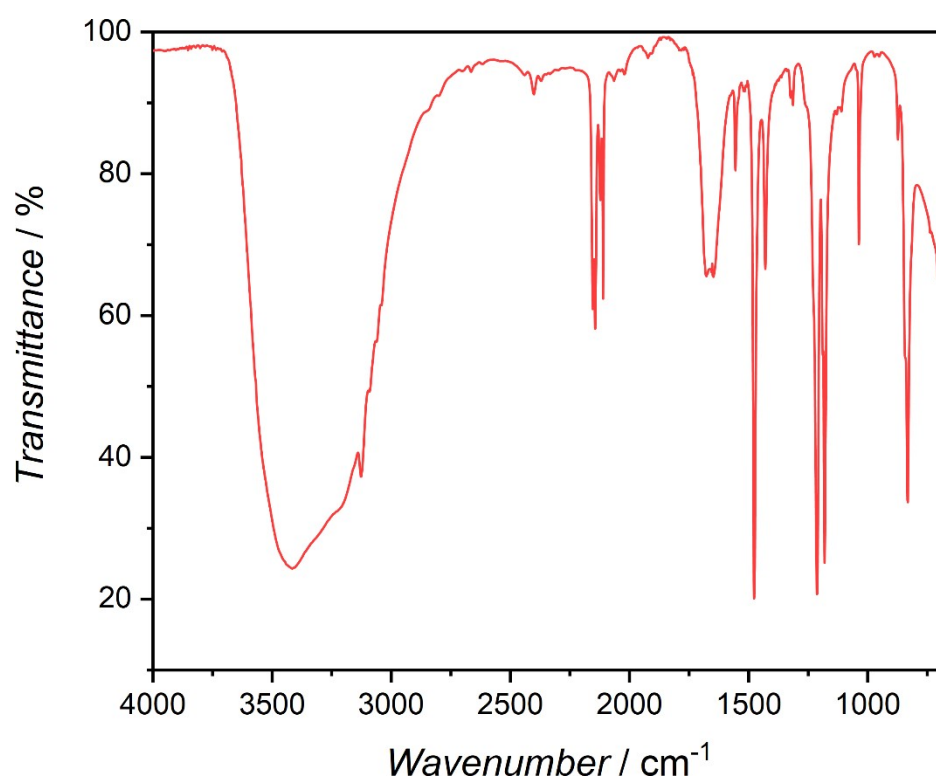


**Figure S6.** Infrared spectrum obtained for  $\text{Fe}_2\text{Nb}$ .

**Table S1.** Crystallographic data obtained from SCXRD for **Fe<sub>2</sub>Mo**, **Fe<sub>2</sub>W** and **Fe<sub>2</sub>Nb**.

	<b>Fe<sub>2</sub>Mo</b>	<b>Fe<sub>2</sub>W</b>	<b>Fe<sub>2</sub>Nb</b>
CCDC	2155443	2155441	2155442
Formula	C <sub>28</sub> H <sub>36</sub> Fe <sub>2</sub> MoN <sub>12</sub> O <sub>17</sub>	C <sub>28</sub> H <sub>36</sub> Fe <sub>2</sub> N <sub>12</sub> O <sub>17</sub> W	C <sub>28</sub> H <sub>36</sub> Fe <sub>2</sub> N <sub>12</sub> NbO <sub>17</sub>
FW / g mol <sup>-1</sup>	1020.33	1108.24	1017.30
Temperature / K	120(2)	120(2)	100(2)
Crystal system	monoclinic	monoclinic	monoclinic
Space group	<i>C2/c</i>	<i>C2/c</i>	<i>C2/c</i>
<i>a</i> / Å	12.9910(6)	12.9768(3)	13.0334(3)
<i>b</i> / Å	20.3836(9)	20.3701(5)	20.5187(3)
<i>c</i> / Å	15.7673(7)	15.7622(6)	16.0049(2)
$\beta$ / °	101.721(2)	101.844(1)	102.618(2)
<i>V</i> / Å <sup>3</sup>	4088.2(3)	4077.9(2)	4176.79(13)
<i>Z</i>	4	4	4
$\rho_{\text{calc}}$ / g cm <sup>-3</sup>	1.658	1.805	1.618
Abs. coeff. / mm <sup>-1</sup>	1.087	3.601	0.901
<i>F</i> (000)	2072	2200	2068
Radiation source	Mo K $\alpha$	Mo K $\alpha$	synchrotron ( $\lambda$ = 0.6754 Å)
Crystal size / mm	0.05 x 0.05 x 0.32	0.04 x 0.04 x 0.25	0.01 x 0.01 x 0.05
$\theta$ range / °	3.31-24.73	3.31-24.49	1.79-23.91
Reflections collected	23780	20717	16916
<i>R</i> <sub>int</sub>	0.045	0.036	0.050
Parameters/restraints	315/21	315/21	315/21
<i>GOF</i> on <i>F</i> <sup>2</sup>	1.10	1.15	1.05
<i>R</i> <sub>1</sub> (refl. with <i>I</i> > 2 $\sigma$ ( <i>I</i> ))	0.030	0.023	0.052
<i>wR</i> <sub>2</sub> (all reflections)	0.072	0.045	0.149
Largest diff. peak and hole / e Å <sup>-3</sup>	0.85/-0.64	0.64/-1.00	1.25/-2.28

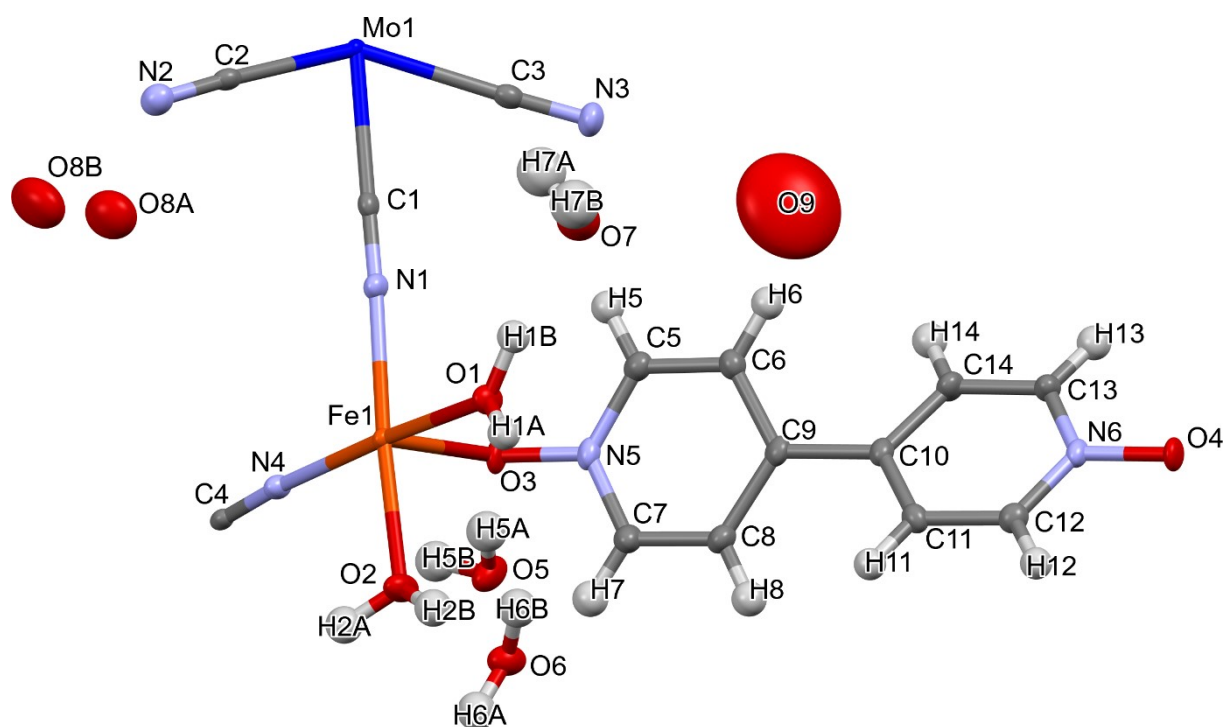


**Figure S7.** Asymmetric unit of **Fe<sub>2</sub>Mo** at 120(2) K. Thermal ellipsoids are demonstrated at 50% probability level.

**Table S2.** Continuous symmetry measures.

	<b>TDD</b>	<b>SAPR</b>	<b>BTPR</b>	<b>OC</b>	<b>TPR</b>
<b>Fe<sub>2</sub>Mo</b> (Mo)	0.219	1.939	2.000	---	---
<b>Fe<sub>2</sub>Mo</b> (Fe)	---	---	---	0.187	14.900
<b>Fe<sub>2</sub>W</b> (W)	0.206	1.962	2.000	---	---
<b>Fe<sub>2</sub>W</b> (Fe)	---	---	---	0.189	14.925
<b>Fe<sub>2</sub>Nb</b> (Nb)	0.174	2.021	1.934	---	---
<b>Fe<sub>2</sub>Nb</b> (Fe)	---	---	---	0.162	14.920

**TDD** – triangular dodecahedron, **SAPR** – square antiprism, **BTPR** – biaugmented trigonal prism, **OC** – octahedron, **TPR** – trigonal prism.

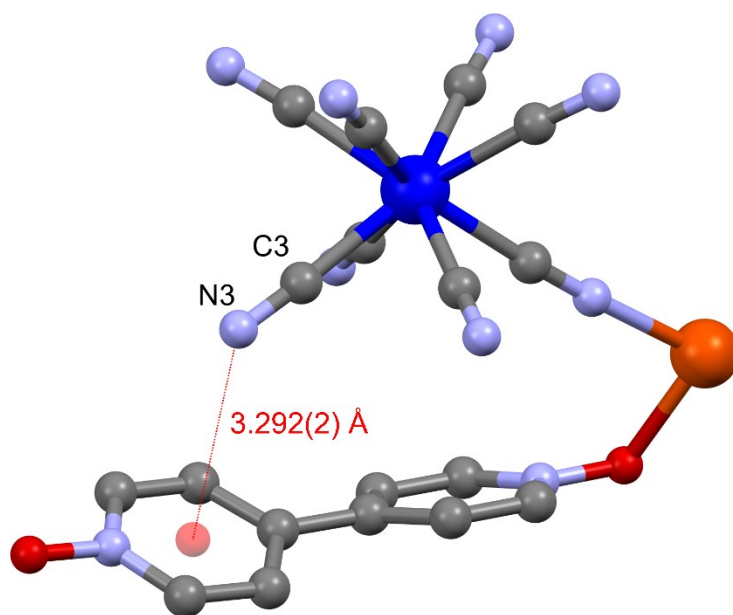


**Figure S8.** Fragment of crystal structure of **Fe<sub>2</sub>Mo** demonstrating a anion- $\pi$  contact between the cyanido ligand and a centroid of 4,4'-bpdo aromatic ring.

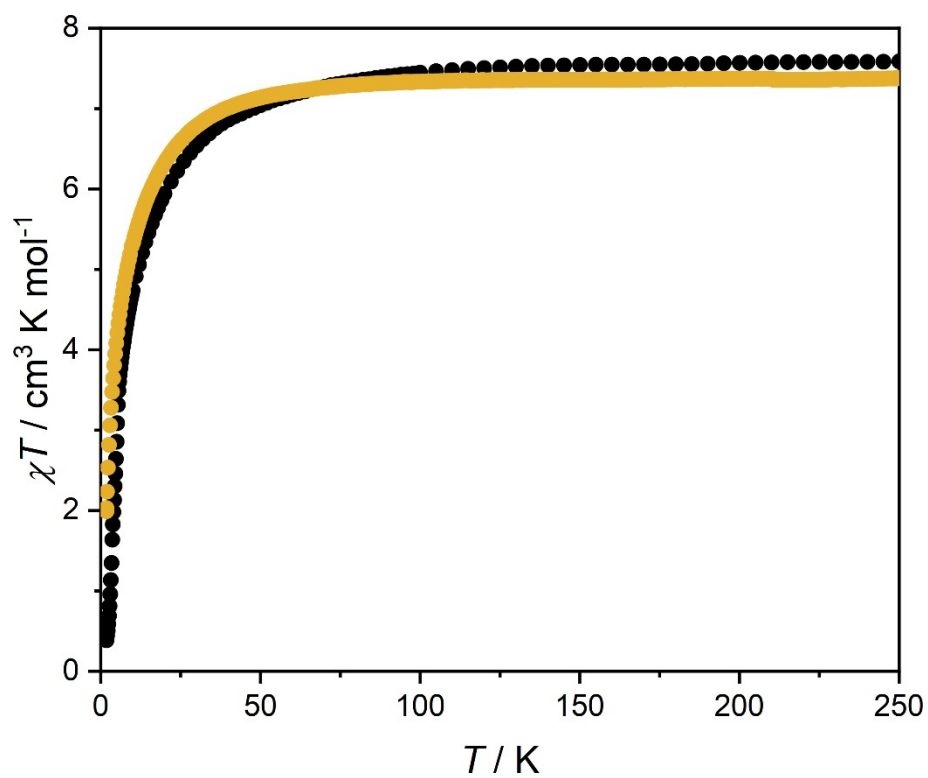


**Figure S9.** Comparison of  $\chi T(T)$  curves recorded at 0.1 T for **Fe<sub>2</sub>Nb** (black points) and **Fe<sub>2</sub>Mo** (yellow points).



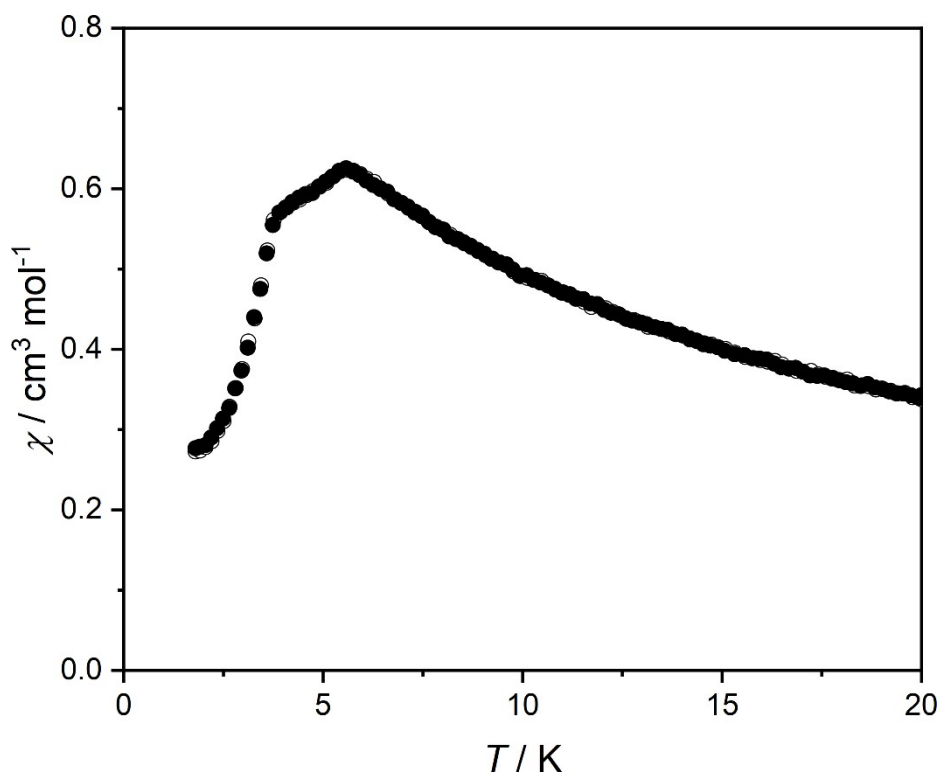


**Figure S10.** Zfc (open circles) – fc (full circles) curves recorded for **Fe<sub>2</sub>Nb** under  $H_{DC} = 0.00035$  T.

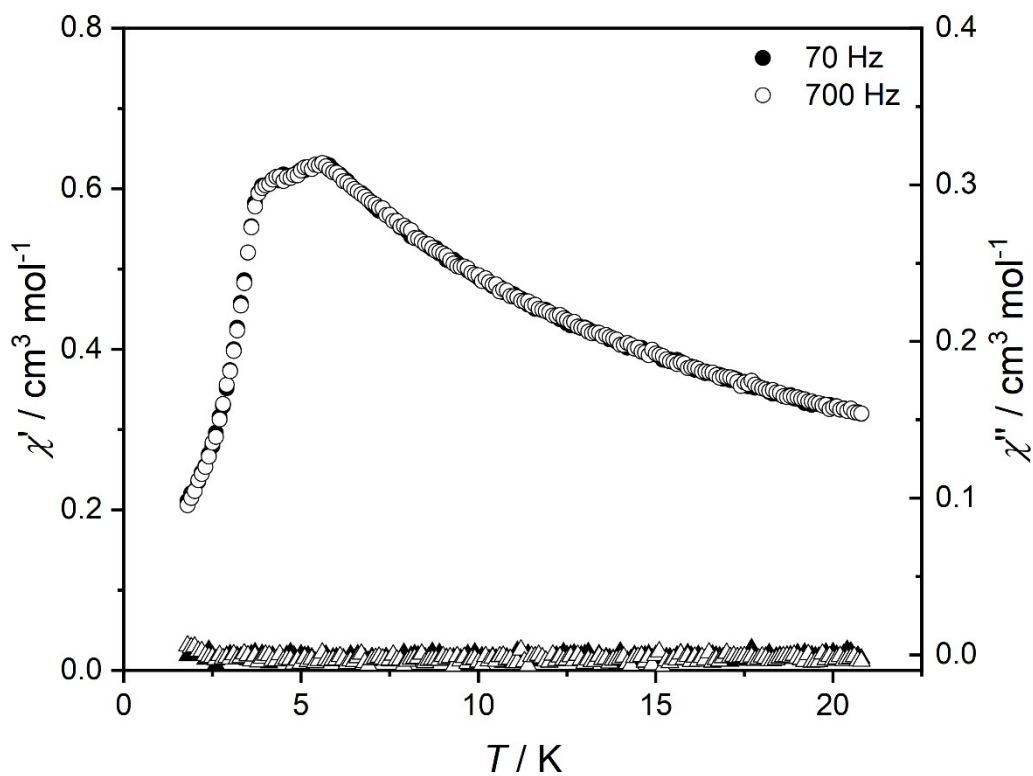


**Figure S11.** Temperature dependence of  $\chi'$  (circles) and  $\chi''$  (triangles) recorded for **Fe<sub>2</sub>Nb** under  $H_{DC} = 0$  T and  $H_{AC} = 0.0001$  T.

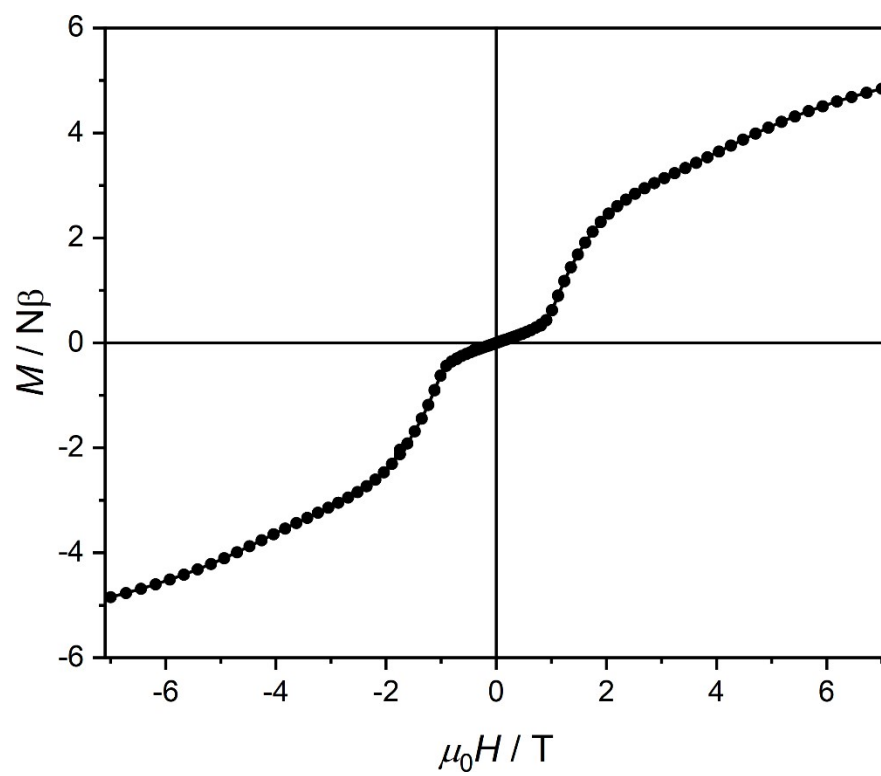


**Figure S12.** Magnetic field dependence of magnetization recorded for  $\text{Fe}_2\text{Nb}$  at 1.8 K.

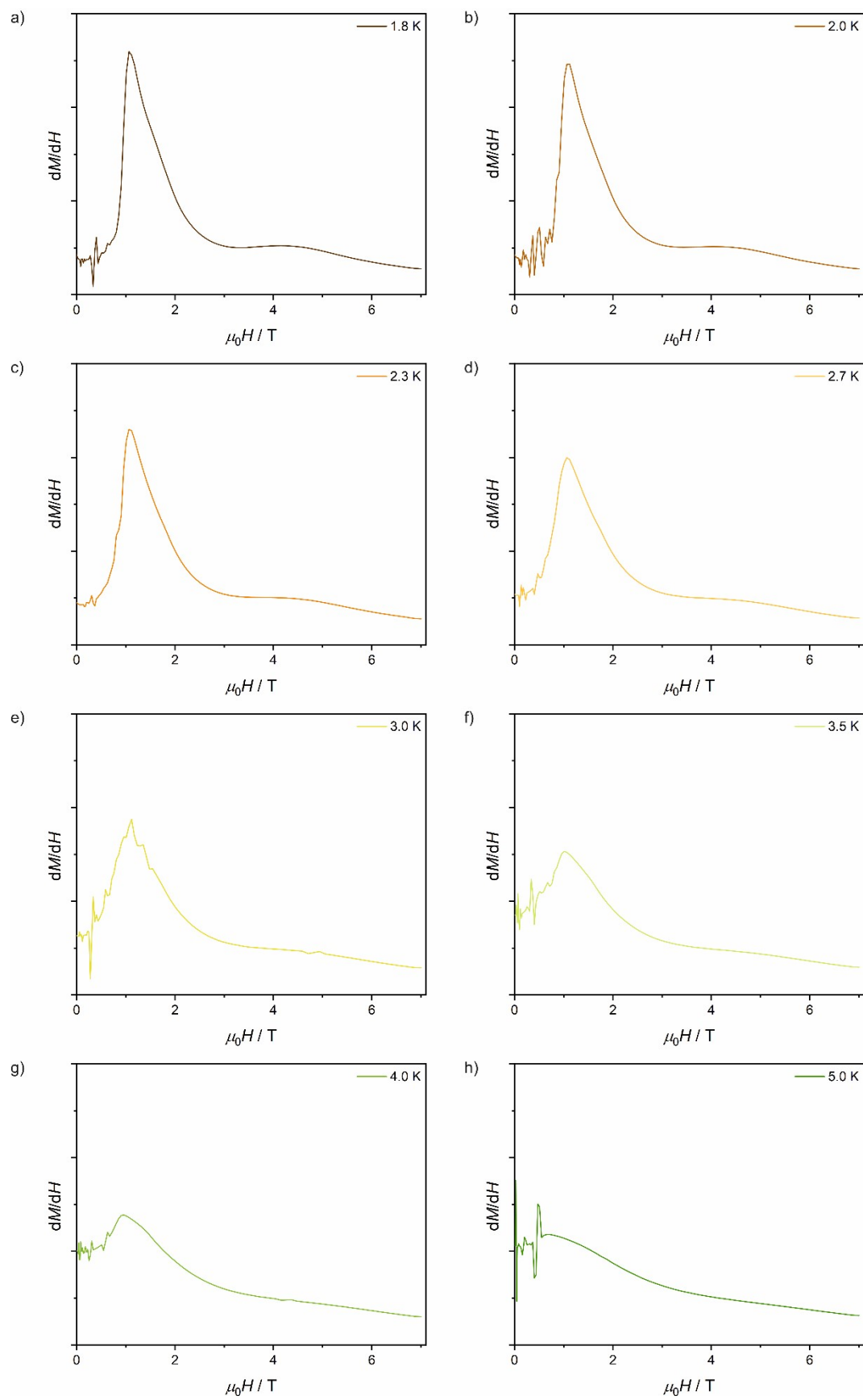


**Figure S13.** Derivatives of magnetisation versus field curves for  $\text{Fe}_2\text{Nb}$ .

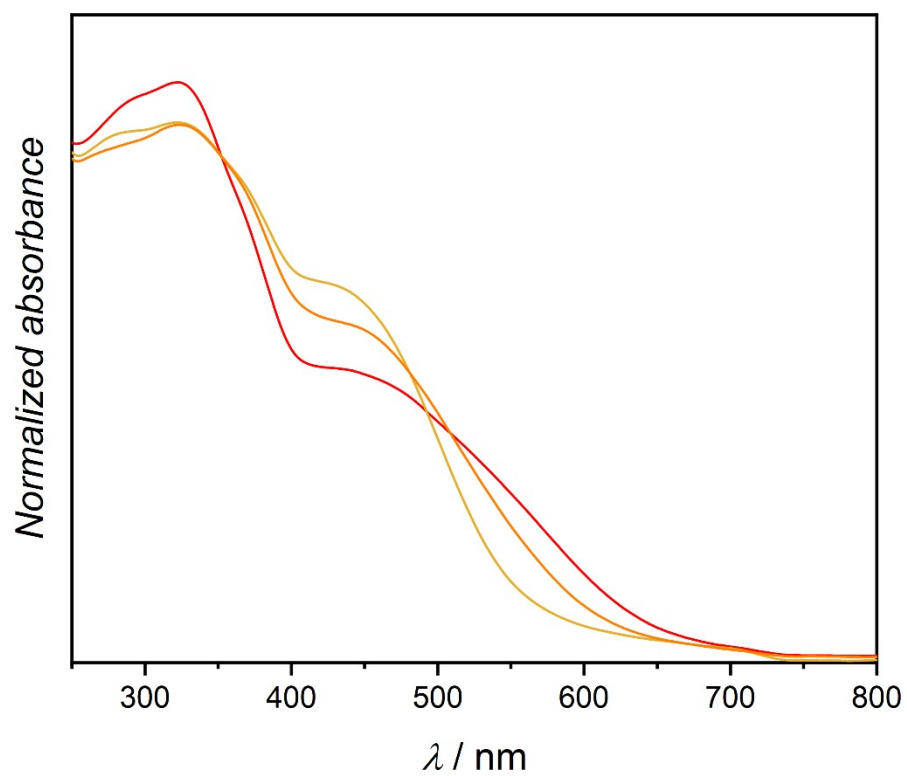


**Figure S14.** Solid state UV-vis spectra for **Fe<sub>2</sub>Nb** (red), **Fe<sub>2</sub>Mo** (yellow) and **Fe<sub>2</sub>W** (orange) obtained at room temperature.

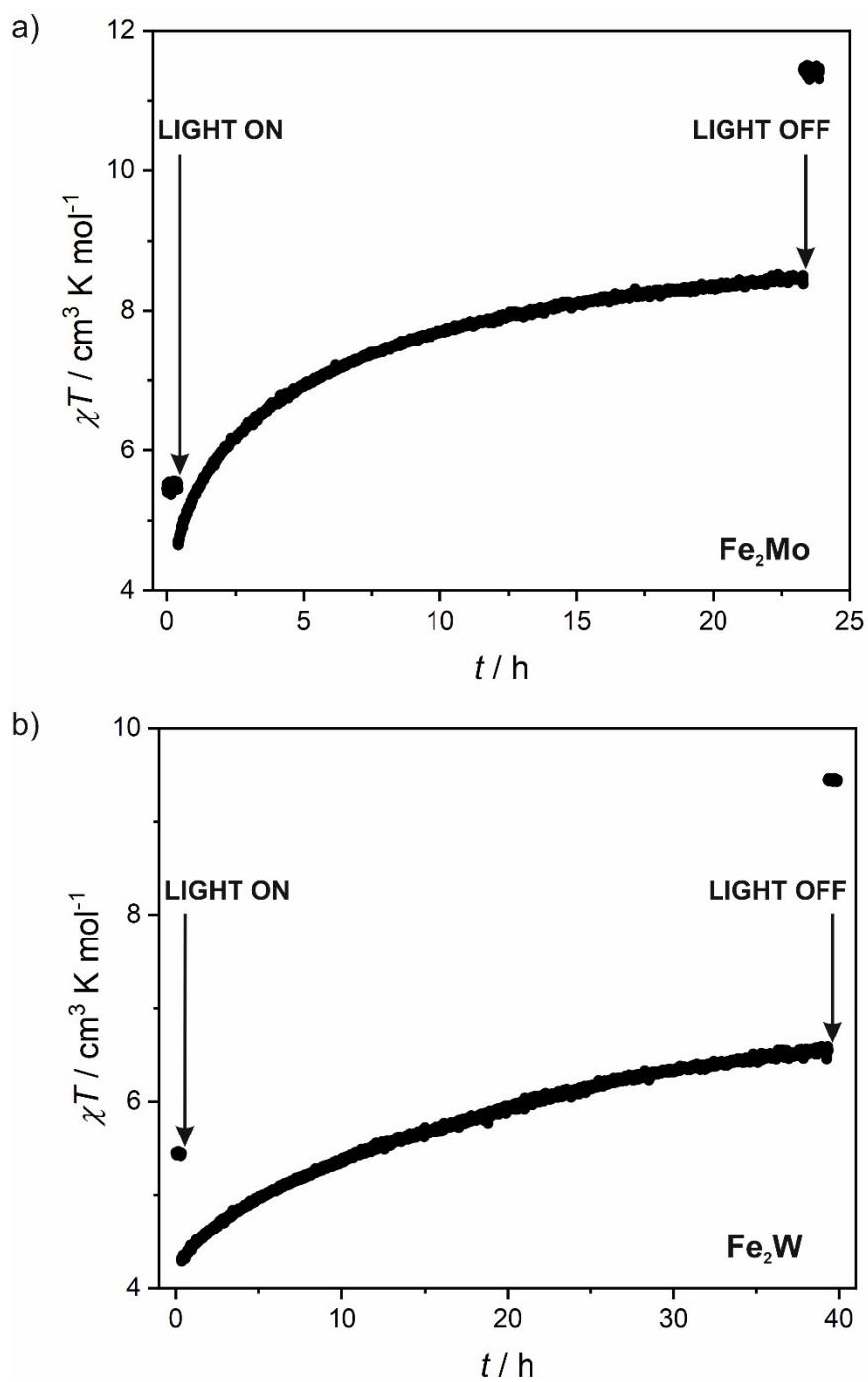


**Figure S15.**  $\chi T(t)$  curves obtained for  $\text{Fe}_2\text{Mo}$  (a) and  $\text{Fe}_2\text{W}$  (b) upon 450 nm light irradiation at 10 K and  $H_{\text{DC}} = 0.005$  T.

## References

1. G. Sheldrick, *Acta Crystallogr. A*, 2008, **64**, 112-122.
2. G. Sheldrick, *Acta Crystallogr. A*, 2015, **71**, 3-8.
3. O. V. Dolomanov, L. J. Bourhis, R. J. Gildea, J. A. K. Howard and H. Puschmann, *J. Appl. Crystallogr.*, 2009, **42**, 339-341.
4. C. F. Macrae, I. Sovago, S. J. Cottrell, P. T. A. Galek, P. McCabe, E. Pidcock, M. Platings, G. P. Shields, J. S. Stevens, M. Towler and P. A. Wood, *J. Appl. Crystallogr.*, 2020, **53**, 226-235.